0022-3565/07/3212-492–500$20.00
THE JOURNAL OF PHARMACOLOGY AND EXPERIMENTAL THERAPEUTICS
Vol. 321, No. 2
116459/3198765
Printed in U.S.A.

JPET 321:492–500, 2007

Hyperforin Blocks Neutrophil Activation of Matrix Metalloproteinase-9, Motility and Recruitment, and Restrains Inflammation-Triggered Angiogenesis and Lung Fibrosis

Isabella Dell'Aica, Raffaele Niero, Francesco Piazza, Anna Cabrelle, Luigi Sartor, Cristiano Colalto, Enrico Brunetta, Girieca Lorusso, Roberto Benelli, Adriana Albini, Fiorella Calabrese, Carlo Agostini, and Spiridione Garbisa

Department of Experimental Biomedical Sciences, Medical School, Padova, Italy (I.D.A., L.S., C.C., S.G.); Venetian Institute of Molecular Medicine, Padova, Italy (R.N., F.P., A.C., E.B., C.A.); Department of Clinical and Experimental Medicine, Medical School, Padova, Italy (F.P., A.C., E.B., C.A.); IRCCS Multimedica, Milano, Italy (G.L., A.A.); Molecular Biology Laboratory, National Institute for Research on Cancer, Genova, Italy (R.B.); and Department of Pathology, Medical School, Padova, Italy (F.C.)

Received October 31, 2006; accepted February 6, 2007

ABSTRACT

Hyperforin (Hyp), a polyphenol-derivative of St. John's wort (*Hypericum perforatum*), has emerged as key player not only in the antidepressant activity of the plant but also as an inhibitor of bacteria lymphocyte and tumor cell proliferation, and matrix proteinases. We tested whether as well as inhibiting leukocyte elastase (LE) activity, Hyp might be effective in containing both polymorphonuclear neutrophil (PMN) leukocyte recruitment and unfavorable eventual tissue responses. The results show that, without affecting in vitro human PMN viability and chemokine-receptor expression, Hyp (as stable dicyclohexylammonium salt) was able to inhibit in a dose-dependent manner their chemotaxis and chemoinvasion (IC_{50} = 1 μM for both); this effect was associated with a reduced expression of the adhesion molecule CD11b by formyl-Met-Leu-Phe-stimulated neutrophils and block of LE-triggered activation of the gelatinase matrix metalloproteinase-9. PMN-triggered angiogenesis is also blocked by both local injection and daily i.p. administration of the Hyp salt in an interleukin-8-induced murine model. Furthermore, i.p. treatment with Hyp reduces acute PMN recruitment and enhances resolution in a pulmonary bleomycin-induced inflammation model, significantly reducing consequent fibrosis. These results indicate that Hyp is a powerful anti-inflammatory compound with therapeutic potential, and they elucidate mechanistic keys.

St. John's wort (*Hypericum perforatum*) extracts are a rich source of unique natural products, and prenylated acylphloroglucinol hyperforin (Hyp) has emerged as key player in the antidepressant activity of the plant (Barnes et al., 2001). However, it also exerts remarkable antibiotic activity against several Gram-positive bacteria, including methicillin-resistant *Staphylococcus aureus* (Schempp et al., 1999), and it has an antiproliferative effect in vitro in phytohemagglutinin-stimulated blood lymphocytes (Schempp et al., 2000) as well as in several tumor cell lines, where it also inhibits proliferation in vivo (Schempp et al., 2002).

The pharmacokinetics of Hyp has been thoroughly investigated, and it has revealed that the compound is bioavailable upon oral ingestion, with antidepressive therapeutic doses of St. John's wort leading to serum levels of 0.45 μM (Biber et al., 1998). We have demonstrated that at this concentration Hyp is a good inhibitor of leukocyte elastase (LE), exerts strong inhibition of in vitro tumor cell chemoinvasion, and in vivo produces remarkable reduction of neovascularization, size of experimental colon carcinoma metastases, and inflammatory tumor infiltration (Donà et al., 2004). The

This work was supported by grants from the Associazione Italiana per la Ricerca sul Cancro, Fondo per gli Investimenti della Ricerca di Base-Ministero dell'Istruzione, dell'Università e della Ricerca, and Programmi di Ricerca di Interesse Nazionale-Ministero dell'Istruzione, dell'Università e della Ricerca Italian Government, University of Padova, and "Compagnia di San Paolo" project 1958StS/fs, Italy. G.L. is in the "Degenerative Disease and Immunopathology" Ph.D. program at the Medical School, University of Insubria, Varese, Italy.

Article, publication date, and citation information can be found at http://jpet.aspetjournals.org.

doi:10.1124/jpet.106.116459.

ABBREVIATIONS: Hyp, hyperforin; LE, leukocyte elastase; PMN, polymorphonuclear leukocyte; ECM, extracellular matrix; MMP, matrix metalloproteinase; Hyp-DCHA, dicyclohexylammonium salt of hyperforin; DMSO, dimethyl sulfoxide; fMLF, *N*-formyl-Met-Leu-Phe; BM, basement membrane; DMEM, Dulbecco's modified Eagle's medium; MFI, mean fluorescence intensity; IL, interleukin; PBS, phosphate-buffered saline; BAL, bronchoalveolar lavage; H&E, hematoxylin and eosin; MP, mean percentage.

latter finding, and the recently reported modulation of immune inflammatory responses in intestine and liver (Zhou et al., 2004), led us to investigate in more detail the effects of Hyp on the major cellular component of the inflammatory compartment—the polymorphonuclear neutrophil (PMN) leukocytes—and on their lytic capabilities.

PMNs are the major source of LE, and they act both intracellularly to kill engulfed pathogens and extracellularly as mediator of coagulation, immune responses, and wound debridement (Sternlicht and Werb, 1999). Because LE has the potential to degrade some structural proteins of the extracellular matrix (ECM), such as elastin, fibronectin, and collagens, excess LE activity has been involved in several pathological conditions leading to impairment of ECM organization, including rheumatoid arthritis, emphysema, cystic fibrosis (Sternlicht and Werb, 1999), and tumor progression (Balkwill and Mantovani, 2001). LE also activates the proenzymatic form of matrix metalloproteinase (MMP)-9 (Sternlicht and Werb, 1999) massively released by the PMNs and instrumental to degradation of matrix components (Delclaux et al., 1996; Esparza et al., 2004).

Here, we tested whether the Hyp-triggered inhibition of LE activity might advantageously develop into containment of both PMN recruitment and any unfavorable downstream tissue responses. Hyp, a mixture of interconverting tautomers, is prone to air oxidation, and it is unstable in most organic solvents. Its stable and crystalline dicyclohexylammonium salt (Hyp-DCHA; Fig. 1) (Chatterjee et al., 1999; Verotta et al., 2002) is a convenient storage form of the natural product, already used in studies of antidepressant activity in rats (Cervo et al., 2002) and antitumor invasion in mice (Donà et al., 2004); thus, it was chosen for our investigation. Here, we show that Hyp-DCHA restrains PMN chemotaxis and chemoinvasion, and protects against inflammatory events taking place in animal models of angiogenesis and bleomycin-induced lung fibrosis.

Materials and Methods

Materials. The stable and crystalline dicyclohexylammonium salt of hyperforin, used in all experiments (Hyp-DCHA in Fig. 1), was prepared by Prof. G. Appendino (University of Piemonte Orientale, Novara, Italy) according to the method described in patent PCT WO 99/41220 (Chatterjee et al., 1999). Hyp-DCHA was solubilized 10 mM in DMSO, and the dilutions used never exceeded 1% DMSO final concentration (DMSO was also included in appropriate controls without Hyp-DCHA), except in the in vivo experiments where 150 μl i.p. injections contained 10% DMSO (see below).

Cytochalasin B and formyl-Met-Leu-Phe (fMLF) were from Sigma-Aldrich (St. Louis, MO), fetal calf serum was from Biochrom (Berlin, Germany), basement membrane (BM) matrix (Matrigel) was from Becton Dickinson (Bedford, MA), polyvinylpyrrolidone-free polycarbonate filters were from Millipore (Billerica, MA), Ficoll-Paque Plus (<0.12 enzyme unit/ml) was from Amersham Biosciences (Milan, Italy), and okadaic acid was from Calbiochem (Darmstadt, Germany). Fluorescein isothiocyanate-conjugated anti-CXCR1, -CXCR2, -CXCR3, -CCR3, -CCR5, and -CCR7 antibodies and phycoerythrin-conjugated anti-CXCR4, -CXCR6, -CCR1, -CCR2, and -CCR6 antibodies were from R&D Systems (Minneapolis, MN). Fluorescein isothiocyanate-conjugated anti-CD11a, -CD18, and phycoerythrin-conjugated anti-CD62L, -CD11b were from Becton Dickinson (Sunnyvale, CA). All of the other reagents, if not specified, were purchased from Sigma-Aldrich.

Neutrophil Isolation. Human PMNs were isolated, >96% pure, from buffy coats of healthy donors, as described previously (Dri et al., 1999).

MMP-9 Activation. PMNs in serum-free medium (Dulbecco's modified Eagle's medium; DMEM) were preincubated 15 min with or without micromolar Hyp-DCHA, activated by fMLF/cytochalasin, and incubated 4 h at 37°C. The conditioned medium was then analyzed by gelatin zymography, as follows. Unheated samples were electrophoresed in 0.1% gelatin-containing 6% polyacrylamide, in presence of SDS. After electrophoresis, the gels were washed twice for 30 min with 2.5% Triton X-100 and then incubated overnight at 37°C in Tris buffer (50 mM Tris-HCl, 200 mM NaCl, and 10 mM $CaCl_2$, pH 7.4). The gels were then stained with 30% methanol/10% acetic acid containing 0.5% Coomassie Brilliant Blue R-250, and they were destained in the same solution without dye. Clear bands of gelatinolysis on the blue background were quantitated using an image analyzer system with Gel-Doc 2000 and QuantityOne software (Bio-Rad, Hercules, CA).

PMN Chemotaxis and Chemoinvasion. Human PMN response to 10^{-7} M fMLF or 50 ng/ml IL-8 was measured by seeding 2×10^6 cells, in serum-free medium with or without Hyp-DCHA, onto the top compartment of 8-mm-diameter Boyden chambers; 5-μm pore-size filters, uncoated or coated with gelatin (chemotaxis) or Matrigel (chemoinvasion), were separating the bottom compartment filled with medium containing one (or none) of the above-mentioned chemoattractants; after 40 or 120 min at 37°C, respectively, migrated cells were collected and counted under a microscope (Benelli et al., 2000).

PMNs were also seeded (5×10^5) onto 96-well plates, incubated in 5% CO_2, air at 37°C in 90 μl of DMEM without phenol red and fetal calf serum, and with or without Hyp-DCHA. After 4 and 20 h, the viability was determined by CellTiter 96® colorimetric assay (Promega, Madison, WI), which measures the conversion of a tetrazolium

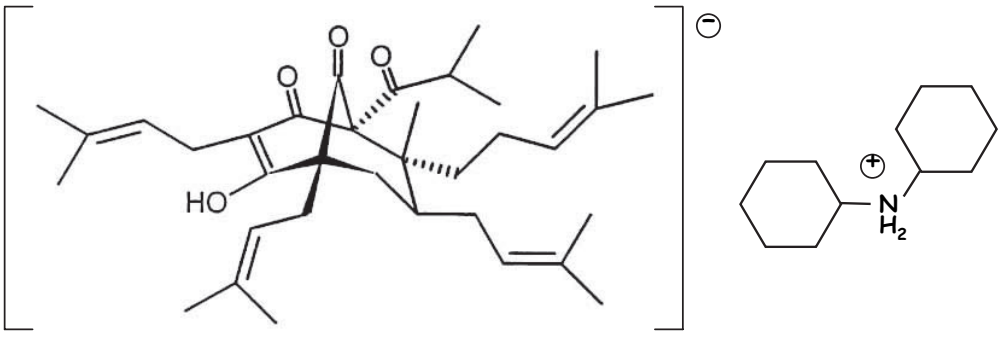

Hyp-DCHA

Fig. 1. Molecular structure of the prenylated acylphloroglucinol dicyclohexylammonium salt, Hyp-DCHA, used in this investigation.

compound "presumably by NADPH or NADH produced by dehydrogenase enzymes in metabolically active cells".

PMN Cytofluorimetry. PMNs were suspended in 20 ml of DMEM in a 50-ml Falcon tube rotated upside-down at 15 rpm for 1 h at 37°C (during this treatment, the PMNs released most of their proteolytic and oxidative load), and then they were resuspended in DMEM and incubated for 40 min with or without 10^{-7} M fMLF, 0.3 or 3 μM Hyp-DCHA, and fMLF plus Hyp-DCHA. Cells were centrifuged and incubated 30 min at 22°C with the appropriate antibody, pelleted, and resuspended in PBS. The expression of chemokine receptors or integrins was determined using monoclonal antibodies against CXCR1, CXCR2, CXCR3, CXCR4, CXCR6, CCR1, CCR2, CCR3, CCR5, CCR6, CCR7, CD62L, CD11a, CD11b, and CD18. The effect of Hyp-DCHA was determined by overlaying the flow cytometry histograms of the untreated, fMLF-treated, and fMLF- plus Hyp-DCHA-treated samples. Cells were scored using a FACSCalibur analyzer (Becton Dickinson), and data were processed using Macintosh CellQuest software program (Becton Dickinson). For each marker, the threshold of positivity was found beyond the nonspecific binding observed in the presence of irrelevant control antibody. Mean fluorescence intensity (MFI) values were obtained by subtracting the MFI of the isotype control from that of the positively stained sample. The differences between the cell peaks were analyzed by the Kolmogorov-Smirnov test, in accordance with the Macintosh CellQuest software user's guide (Becton Dickinson), with index of similarity [D/s (n)] values >10 considered significant.

Inflammation-Triggered Angiogenesis. The following in vivo model of inflammatory angiogenesis was used (Benelli et al., 2002), following approval by the Ethical Committee of the National Institute for Research on Cancer in Genova, Italy. IL-8 and heparin (50 ng and 13 U/pellet, respectively) were added to liquid Matrigel at 4°C, and 500 μl of this Matrigel suspension was slowly injected s.c. into the flank of C57BL6 mice. In vivo, the gel rapidly forms solid implants, and within a few hours, IL-8 recruits PMNs into the Matrigel, which in 4 days become colonized by neoangiogenesis. Two different protocols were used in duplicate experiment.

For one protocol, four groups of six mice received Hyp-DCHA only once, premixed (1, 3, 9, or 27 μM/pellet) with the Matrigel solution, and six mice were used as control (without Hyp-DCHA). Four days after injection, the gels were collected and weighed; most samples were subjected to analysis of hemoglobin content as described previously (Lee and Downey, 2001); others were paraffin-embedded and stained with hematoxylin and eosin for histological analysis or with a rabbit polyclonal anti-myeloperoxidase antibody for histochemical identification of PMNs.

In the second protocol, 14 mice were injected i.p. (Cervo et al., 2002) with 1 mM Hyp-DCHA (in 150 μl of PBS, 0.4% Tween 80, and 10% DMSO) at 9:30 AM and 6:30 PM every day, starting 24 h before Matrigel injection. Twelve animals received injections of vehicle only. Four days after injection, the gels were analyzed as described above.

Bleomycin-Triggered Inflammation. Bleomycin was instilled intratracheally in 16 male C57BL6 mice (17 g; Charles River, Lecco, Italy) as described previously (Lee and Downey, 2001), following approval by the Ethical Committee of the Medical School of Padova. Bleomycin (1.25 U/ml in sterile PBS) was vortexed extensively before each 100-μl aliquot (5 U/kg) was used. The animals were anesthetized, and intratracheal instillation was performed slowly. A group of eight mice was given i.p. injection of Hyp-DCHA as in the second protocol used for angiogenesis, at 9:00 AM and 6:00 PM for 5 days, starting 3 days before bleomycin instillation. The positive control group of eight mice was treated with the bare vehicle solution. A negative control group of eight mice was instilled with PBS alone. Bronchoalveolar lavage (BAL) fluids were obtained from the lungs of mice 2 days after instillation; this timing was chosen on the basis of preliminary experiments showing that the increase of PMNs reaches its maximum level after 2 to 3 days from instillation (Donà et al., 2003). The mice were sacrificed by CO_2 inhalation, and the lungs were flushed three times with 200 μl of ice-cold heparinized physiological saline solution using a 29-gauge needle. A smear of cells collected in the combined lavage fluid from each animal was prepared with cytospin, and the cells were stained with May-Grunwald/Giemsa. In total, 200 mononuclear phagocytes, PMNs, and lymphocytes were counted under the microscope, and the percentage of each type was calculated.

Bleomycin-Induced Pulmonary Fibrosis. Three groups of eight mice were treated with bleomycin-Hyp-DCHA as described above. The experimental group was given i.p. injection of Hyp-DCHA at 9:00 AM and 6:00 PM every day excluding Sunday, starting 3 days before instillation. Thirty-one days after intratracheal instillation, the mice were weighed, anesthetized, heparinized, and exsanguinated via the femoral artery. The heart and lungs were them removed en bloc. Lungs were fixed by intratracheal perfusion of 10% formalin at a constant pressure of 25 cm H_2O for 24 h. The lungs were dissected away from the external vasculature and bronchi, and they were sectioned parasagittally, superior to inferior, embedded in paraffin, sectioned at 5 μm, and stained with H&E and Heidenhain trichrome. The inflammatory cell infiltration, interstitial fibrosis, and alveolar cuboidalization were evaluated using a semiquantitative analysis with a percentage value of parenchyma involved. Heart, liver, and kidney were also histologically processed to detect any toxic pathological changes.

Fibrosis was also measured by computerized morphometry using an image analyzer system, with Image-Pro Plus software, version 4.1 (Media Cybernetics, Inc., Silver Spring, MD) as described previously (Donà et al., 2004). At least 10 fields at 20-fold magnification were randomly measured selecting lung parenchyma and perivascular/conducting airway structures in fibrotic areas. The analyses were performed blind by an experienced pathologist (F.C.). Slides from the three groups of mice were randomized, coded, and examined without knowledge of the treatment. The experiment was repeated twice.

Measurement of Hyp Blood Level. For determination of Hyp level, blood samples were obtained from mice 30 min after injection of Hyp as described above (hematic peak) (Cervo et al., 2002), and Hyp in the plasma was identified and quantified by high-performance liquid chromatography as reported previously (Brolis et al., 1998; Donà et al., 2004).

Determination of Hydroxyproline. The hydroxyproline content of mouse lung was determined using standard methods (Christensen et al., 1999), with slight modifications. After rinsing with PBS, the upper left lung lobe was defatted, dried, weighed, and hydrolyzed 22 h at 110°C in 6 N HCl. Aliquots were then assayed by adding chloramine T solution for 20 min, 3.15 M perchloric acid for 5 min, and Erlich's reagent at 60°C for 20 min. Absorbance was measured at 561 nm, and the amount of hydroxyproline was determined against a standard curve.

Statistics. Data are expressed as the means of three determinations for biochemical assays and six for migration and invasion (four PMN donors separately). The results of the IL-8-triggered angiogenesis were analyzed using the Mann-Whitney U test. Comparisons of BAL cell population and hydroxyproline content were conducted by one-way analysis of variance, with significance set at $p < 0.05$. For morphometric analysis of lung tissue, 10 fields from complete left lung of each animal were examined, and the data of each group averaged; comparisons were conducted by one-way analysis of variance, with significance set at $p < 0.05$.

Results

Activation of MMP-9. Micromolar Hyp-DCHA, added to PMNs 15 min before fMLF/cytochalasin-triggered activation, produced dose-dependent inhibition of the MMP-9 activation taking place over the after 4 h of incubation. The example experiment in Fig. 2 shows a 49% reduction at 1 μM Hyp (lane 3), and 75% at 4 μM (lane 4); this inhibition was

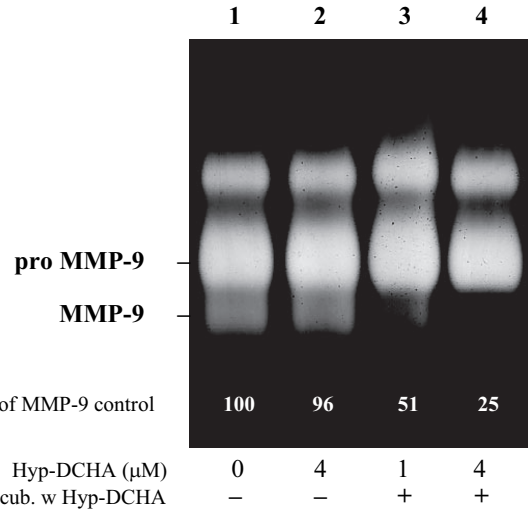

Fig. 2. Hyperforin (as Hyp-DCHA) dose-dependently prevents PMN MMP-9 activation. Gelatin-zymography of medium conditioned 4 h by fMLF/cytochalasin-activated PMNs shows a major band of pro-MMP-9 gelatinolytic activity and a lower minor band of MMP-9 activated form, which (in PMN-conditioned medium) is typically diffused; 15-min preincubation of PMNs with μM Hyp-DCHA prevents, in a dose-dependent manner, the proteolytic processing of the zymogen to the activated form (lanes 3 and 4). White numbers refer to the densitometric values of MMP-9 activated form (compared with control 100%); example of triplicate experiments.

maintained over the following 4 h at 37°C (data not shown). When added at the time of PMN activation, Hyp-DCHA failed to significantly restrain the proteolytic processing on pro-MMP-9 (lane 2).

Chemotaxis and Chemoinvasion. The effect of Hyp-DCHA on PMN migration toward the bacterial tripeptide fMLF or IL-8 was measured by a modified Boyden chamber assay. In both chemotaxis and chemoinvasion assays, PMNs showed a 2-fold increase in migration to the chemoattractant over nonstimulated controls, and the presence of μM Hyp-DCHA resulted in a down-modulatory effect (Fig. 3).

On gelatin-coated filters (chemotaxis), Hyp-DCHA down-modulated PMN chemotaxis, within the range of concentrations tested (0–4.5 μM), with an $IC_{50} = 1$ μM (Fig. 3A). Parallel assays without gelatin gave similar dose-response results, with an $IC_{50} < 0.5$ μM (data not shown). Controls with Hyp-DCHA in the bottom chamber excluded any possible chemotactic activity of the compound (data not shown). On filters coated with basement membrane matrix Matrigel (chemoinvasion), the invasive capacity of PMNs toward the chemoattractant was restrained in a dose-dependent manner by Hyp-DCHA, with an $IC_{50} < 1$ μM (Fig. 3B). At this concentration, the PMN short-term viability (4 and 20 h) was not significantly affected (3 ± 2%) by Hyp-DCHA, whereas it was following 24 h over 10 μM (37 ± 5%).

PMN Receptors and Integrins. The exposure of chemokine receptors and integrins (see *Materials and Methods*) to the cell surface was studied by cytofluorometry: all the antigens tested were generally down-modulated under the chemoattractant fMLF, at levels that were not modified by 40-min exposure to noncytotoxic concentration of Hyp-DCHA (Table 1). The same was found for the CD62L L-selectin (example in Fig. 4A). In the same conditions, the CD18 integrin-component was unaffected by both fMLF and Hyp-DCHA (Fig. 4B). In contrast, the CD11b integrin component

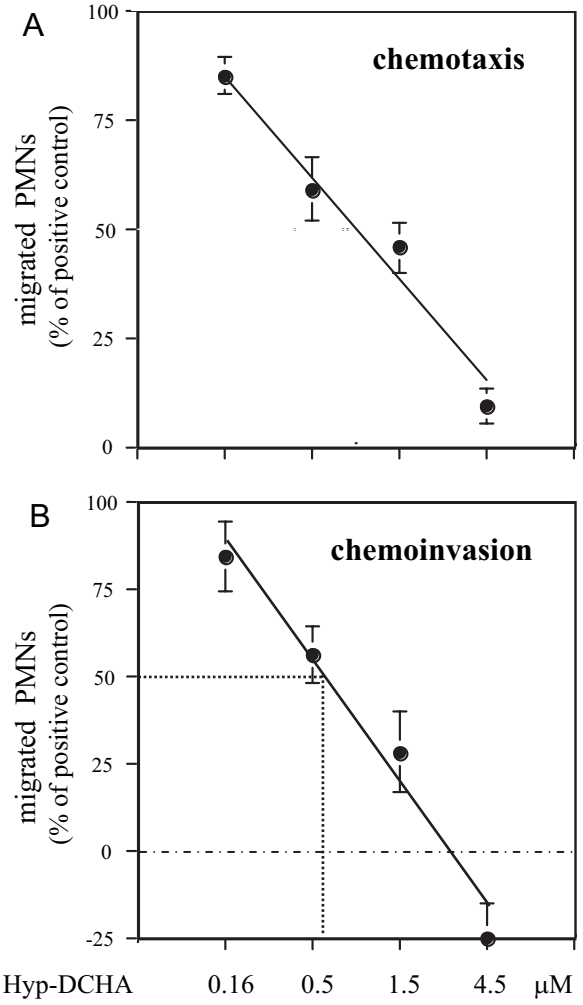

Fig. 3. Hyp-DCHA inhibits both chemotaxis and chemoinvasion of PMNs. The modified Boyden chamber assay shows that PMN chemotaxis through gelatin (A) and chemoinvasion through Matrigel (B) toward fMLF in the bottom chamber is restrained in a dose-dependent manner by the Hyp-DCHA present in the top chamber, with an $IC_{50} = 1$ μM. Equivalent results were obtained using IL-8 as chemoattractant (data not shown). Examples of triplicate experiments (45 min, A; 2 h, B); data are average of quadruplicate measures ± S.D.

was up-modulated by fMLF, but in the presence of Hyp-DCHA this effect was clearly restrained (Fig. 4C).

PMN-Triggered Angiogenesis. Micromolar Hyp-DCHA was effective in restraining IL-8-triggered angiogenesis in the s.c. Matrigel-sponge murine model-system, under two different administration protocols. When mixed with the Matrigel/IL-8 solution before s.c. injection, Hyp-DCHA exerted a dose-dependent inhibition of angiogenesis, with almost complete suppression at 9 μM ($p = 0.02$) (Fig. 5, A–C). When injected i.p. twice per day with a dose already shown to be effective in restraining tumor metastasis in mice (Donà et al., 2004), Hyp-DCHA produced an 80% reduction of the angiogenesis ($p = 0.0001$) (Fig. 5, D–G). This dose did not result in any appreciable side effect, except a nonaggressive increase in the activity of treated mice (as in the next experiment).

Induced Pulmonary Fibrosis. Intraperitoneal administration of the same dose of Hyp-DCHA twice daily for 31 days, starting 3 days before bleomycin treatment, produced some nonmarginal effects even before animal sacrifice: all

TABLE 1

Modulation of chemokine receptors under fMLF and fMLF plus Hyp-DCHA (Hyp)

The expression of all the chemokine receptors was down-modulated or not influenced under fMLF compared with the basal condition, and the 40-min exposure to noncytotoxic Hyp-DCHA concentration did not modify their expression levels (percentages of positive cells and MFI were determined by flow cytometry).

Marker	CXCR1		CXCR2		CXCR3		CXCR4		CXCR6		CCR1		CCR2		CCR3		CCR5		CCR6		CCR7	
	%	MFI	%	MFI	%	MFI	%	MFI	%	MFI	%	MFI	%	MFI	%	MFI	%	MFI	%	MFI	%	MFI
Treatment																						
Basal	98	137	94	28	81	31	68	18	56	6	0	0	35	1	54	6	43	8	0	0	43	5
fMLF	99	98	60	7	64	13	11	5	48	6	0	0	20	1	42	9	50	10	0	0	60	4
fMLF + Hyp	98	87	44	12	63	9	17	7	45	5	0	0	15	1	43	7	30	9	0	0	40	4

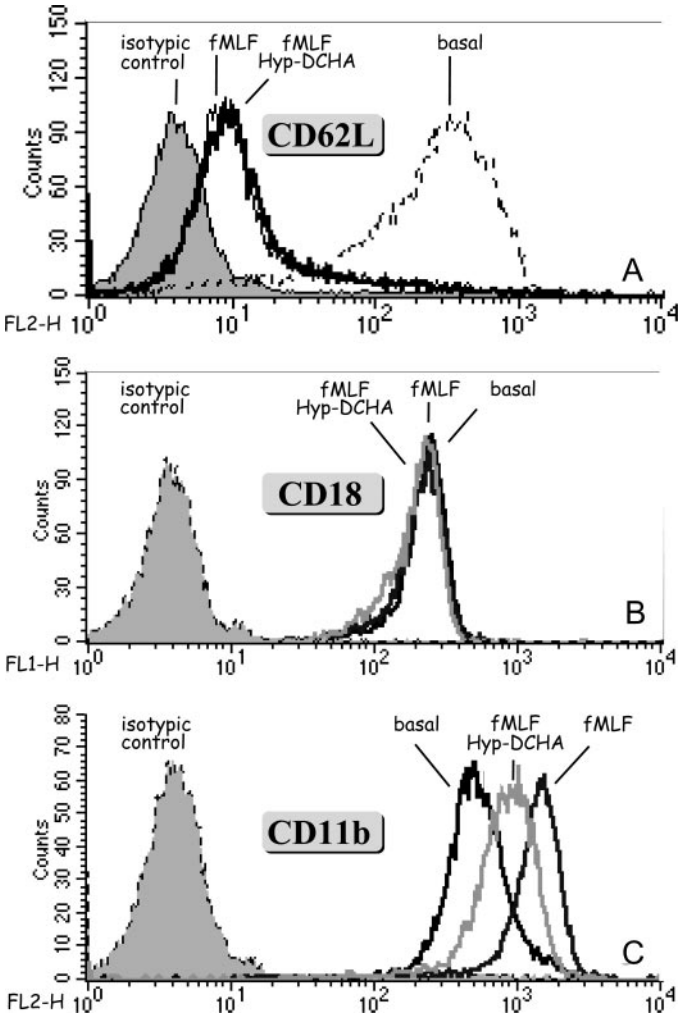

Fig. 4. Cytofluorimetric analysis with antibodies against CD62L, CD18 and CD11b of PMNs pretreated 40 min with 3 μM Hyp-DCHA. The three lines correspond to untreated, fMLF-treated, and fMLF/Hyp-DCHA-treated PMNs; the gray peak refers to the isotypic control. This example of triplicate experiments shows that although Hyp-DCHA does not modify the profile of CD62L- (A) and CD18-positive (B) cells, the compound down-modulates that of CD11b (C) in comparison with PMNs treated with the chemoattractant fMLF alone, as confirmed by the unimodal distribution with a statistically significant shift between the two histograms (D/s = 31.7; $p = 0.001$ according to Kolmogorov-Smirnov test). No Hyp-DCHA-triggered modulation was found with any of the other tested chemokine-receptors or integrins (see *Materials and Methods* for the complete list).

treated mice [(+)-Hyp-DCHA] seemed healthy and more active during the experiment, whereas of the eight positive controls [(−)-Hyp-DCHA] two mice died after 8 to 10 days, and six mice presented signs of dyspnea, ataxia, and characteristic fur changes the second week after treatment. A similar effect was found in a group of animals receiving Hyp-DCHA starting with bleomycin treatment [without the 3-day pretreatment (data not shown)].

The level of Hyp in the blood of treated mice was measured at 30 min after i.p. injection, when the hematic peak is reached (Cervo et al., 2002), and concentrations always <1.2 μM were registered (Donà et al., 2004). At the end of experiment, the (+)-Hyp-DCHA animals registered a weight gain 2.2 times higher than that of the (−)-Hyp-DCHA mice (from 17.0 to 20.0 g and 18.4 g, respectively; $p < 0.01$) and not significantly different from untreated controls.

The potential protective effect of Hyp-DCHA on the bleomycin-induced pathology was thus studied by BAL analysis and histological examination, The inflammatory cell population, examined in BALs obtained 2 days postbleomycin, shows a significantly lower PMN percentage over the total leukocytes in (+)-Hyp-DCHA animals than (−)-Hyp-DCHA controls: the percentage of PMNs falls from 63% of BAL cells without Hyp-DCHA treatment to 28% in animals receiving this treatment, representing a relative decrease of 55%. The difference between mice injected intratracheally with PBS versus bleomycin, and bleomycin versus bleomycin plus i.p. Hyp-DCHA, was significant with $p = 0.0000$ and 0.0003, respectively (Fig. 6).

At 4 weeks, less extensive fibrosis was observed in treated animals than in controls: mean percentage (MP) of lung parenchyma involved 0 versus 13% ($p < 0.02$) (Fig. 7). The severity of inflammation was significantly different (MP 11 versus 36%; $p < 0.02$), whereas no difference was observed for the alveolar changes (cuboidalization) (MP 6 versus 19%; p = N.S.).

To quantitatively determine fibrosis, hydroxyproline content in the lung was measured as a surrogate for lung collagen deposition. Four weeks after bleomycin instillation, the values (mean ± S.E.) were 15.26 ± 0.39, 13.26 ± 0.44, and 12.13 ± 0.17 μg/lobe in (−)-Hyp-DCHA, (+)-Hyp-DCHA, and control animals, respectively, with $p < 0.05$ between the first two groups and $p < 0.01$ between the first and the control. No degenerative changes were observed in heart, liver, and kidney tissue.

Discussion

Inflammatory recruitment entails blood cell transit across the BM underlying the vascular endothelium. An LE-triggered limited proteolysis may activate MMP-9, a gelatinase abundantly secreted by PMNs in zymogen form (Sternlicht and Werb, 1999), that contributes to the degradation of ECM constituents in the area of infiltration, BM structural components included (Delclaux et al., 1996), opening up passageways for PMN extravasation.

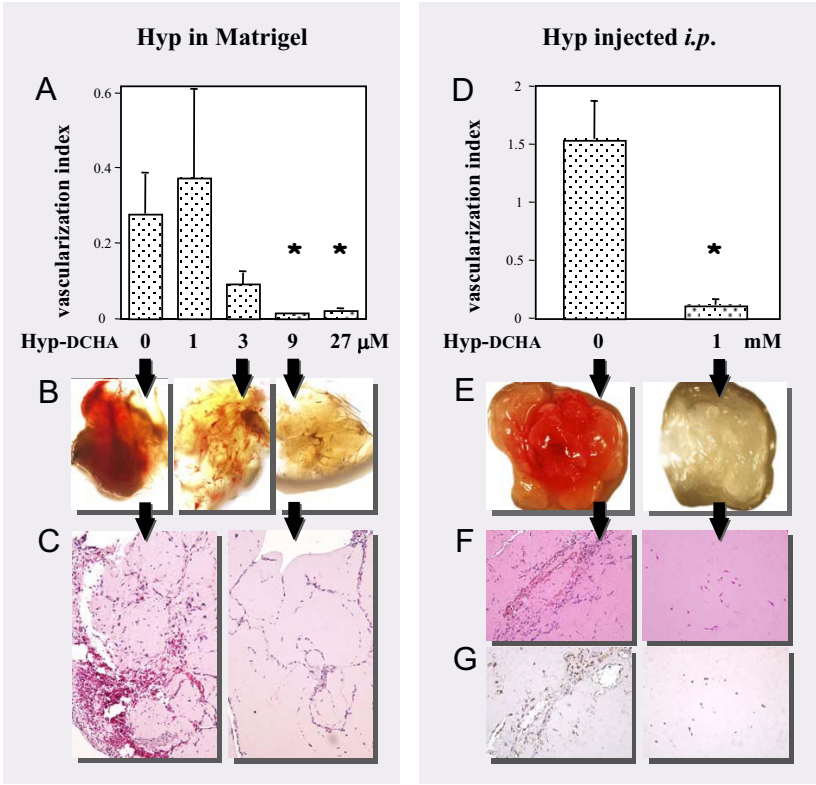

Fig. 5. Hyp-DCHA inhibits PMN-triggered angiogenesis, either when administered once in situ mixed with Matrigel (A–C) or injected daily i.p. (D–G). The histograms (A and D) show the levels of vascularization (± S.E.) into the Matrigel sponges (examples in B and E) after 5 days from s.c. injection. Micrographs of the corresponding sponges stained with H&E (C and F) or anti-myeloperoxidase (G) antibody are shown. *, $p < 0.02$ (A) and $p < 0.0001$ (D) versus control.

We now show that, in the presence of PMNs, micromolar noncytotoxic Hyp-DCHA is efficacious in inhibiting MMP-9 activation. The marked inhibition of LE activity already reported by our group (Donà et al., 2004) substantiates the reported potential of LE to activate MMP-9 in the short-term during PMN recruitment (Delclaux et al., 1996; Sternlicht and Werb, 1999; Esparza et al., 2004). Nevertheless, the lower efficacy of Hyp-DCHA in inhibiting two other proteases secreted by PMNs, cathepsin G (Donà et al., 2004) and protease-3 (data not shown), does not exclude the contribution of other unidentified proteases to MMP-9 activation.

This biochemical evidence led us to suspect that, by hindering a proteolytic machinery, which may facilitate BM penetration and locomotion (Rice and Weiss, 1990), Hyp-DCHA might affect PMN chemotaxis and chemoinvasion. And indeed, the in vitro capacity of human PMNs for migrating toward a chemotactic stimulus, through filters either uncoated or coated with a nonbarrier gelatin matrix (chemotaxis) or with a reconstituted BM barrier (chemoinvasion), was markedly restrained by noncytotoxic micromolar Hyp-DCHA concentrations.

In the chemotaxis assay, gelatin does not represent an obstacle to cell passage, and the restraint in locomotion may involve impairment of chemotactic response and/or adhesion molecules. The cytofluorimetric analysis, a method used to confirm the down-modulatory effect exerted by the chemoattractant fMLF on several chemokine receptors and adhesion molecules (Diaz-Gonzalez et al., 1995), revealed that in the time span used for the chemotaxis assay (40 min), micromolar Hyp-DCHA did not modify the level of all the tested chemokine receptors, or of the expression of CD62L, CD11a, and CD18 adhesion molecules after fMLF priming. The only molecule influenced by the compound was CD11b, which was clearly down-modulated by μM Hyp-DCHA (Fig. 4). Because both CD11a and CD18 expression was found to be unchanged, it is reasonable to hypothesize that the accompanying changes in CD11c levels would account for the maintenance of normal surface amounts of CD18, because it is known that this latter molecule does not exist as a monomer. In this regard, the important issue that derives from our observation surely warrants further investigation. Nevertheless, because CD11b is an adhesion molecule involved in stable attachment of PMNs to endothelial cells and in their extravasation (Luscinskas et al., 1995; Lynam et al., 1998), the down-modulation of this molecule under Hyp-DCHA might be implicated in the inhibition of neutrophil recruitment to inflammation sites.

The reconstituted BM (Matrigel) used in the chemoinvasion assay is a substrate used to mimic the physiological barrier underlying the vascular endothelium that PMNs must cross to extravasate. Our data clearly demonstrate that micromolar Hyp-DCHA blocks the LE-triggered activation of MMP-9 (Sternlicht and Werb, 1999), a gelatinase instrumental to BM traversal (Delclaux et al., 1996, Garbisa et al., 1999) and crucial in the development of fibrosis (Okuma et al., 2004, Corbel et al., 2002). This effect might also contribute to the registered inhibition of PMN invasion under a chemoattractant.

Hyp-DCHA could thus be proposed as an exogenous substitute for direct replacement of α1-protease inhibitor, the endogenous inhibitor most involved in balancing elastolytic burst in inflamed lungs (Sartor et al., 2002). This compound certainly exerts an inhibition superior to a variety of natural and synthetic LE inhibitors: its IC_{50} value is in fact one fourth that reported for the microbial elastatinal (Umezawa, 1976), and 1/5 to 1/20 that of some substituted cephalosporins, β-lactams and trifluoro-methyl ketones, these latter recently suggested for the treatment of diseases character-

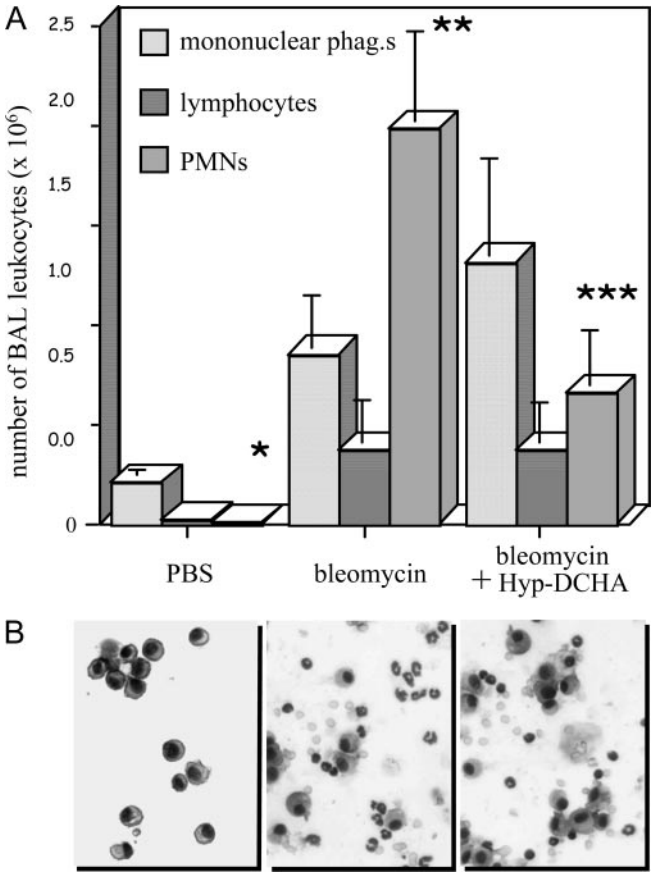

Fig. 6. Daily i.p. Hyp-DCHA restrains PMN recruitment into the lungs of bleomycin-injured mice. A, histogram shows the absolute cell counts (mean of eight mice/group) of three types of inflammatory cells recovered with BAL 2 days after intratracheal injection of PBS, bleomycin, or bleomycin- plus i.p. Hyp-DCHA. * versus **, $p = 0.0000$; ** versus ***, $p = 0.0003$. B, different inflammatory population is documented by example micrographs of the BAL total cell population from the three experimental groups; May-Grunwald/Giemsa staining.

ized by neutrophil and LE involvement (Pacholok et al., 1995).

These initial mechanistic insights encouraged us to investigate whether the effects registered in vitro translate efficaciously in vivo in the restraint of inflammatory cell recruitment. The first approach used a recently optimized model in which the inflammatory infiltrate is responsible for induction of the angiogenic process, in that neutrophil depletion abrogated the angiogenic response induced by CXCR2 ligands (Benelli et al., 2000). Using IL-8 as chemoattractant, we were able to induce a rapid and intense infiltration of neutrophils into Matrigel plugs in mice, accompanied by angiogenesis. Neutrophil recruitment was strongly inhibited both when Hyp-DCHA was injected premixed with the Matrigel plug (only once) and also when it was i.p. injected daily. This in vivo restraint of PMN recruitment is consistent with the in vitro chemotaxis and chemoinvasion results.

The inhibitory effect of Hyp-DCHA on neutrophil migration, in turn, apparently blocks the recruitment of vascular cells in vivo, because angiogenesis was weak or absent in Hyp-DCHA-treated animals. Although a direct effect of the compound on endothelial cells cannot be excluded (as recently reported on Matrigel model; Quiney et al., 2006), the blocking of neutrophil recruitment is paralleled by inhibition of the angiogenic response, as observed in our previous report (Dona et al., 2003). These data indicate Hyp-DCHA as a suitable drug for inhibiting inflammatory angiogenesis, and in turn some severe pathologies such as cancer (Neri and Bicknell, 2005) and pulmonary fibrosis (Burdick et al., 2005), in which angiogenesis may be involved in the development and progression.

A second approach made use of an inflammation-triggered pulmonary fibrosis model system. Chronic inflammation of the alveolar space is thought to mediate the development of pulmonary fibrosis in most interstitial lung disorders; lung damage favors fibroblast proliferation and extracellular matrix remodeling, resulting in irreversible distortion of the lung's architecture (Selman et al., 2001). Intratracheal bleomycin challenge represents a model of acute lymphocyte-dependent lung injury resulting in areas of patchy and chronic inflammation, with release of proteolytic activities and production of cytokines, chemokines, and growth factors that mediate the eventual subpleural, peribronchiolar, and perivascular deposition of extracellular matrix and scar tissue formation that are characteristic of pulmonary fibrosis (Keane et al., 1999). The relationship between inflammation and fibrosis is not clear. Moreover, protection from induced pulmonary fibrosis in chemoattractant chemokine receptor knockout mice (CCR2−/−) was shown to be independent of the magnitude or composition of the inflammatory infiltrate (Moore et al., 2001). More recently, it has also been shown that CCR2 deficiency may improve the outcome of this disease by regulating inflammatory infiltration and macrophage-derived MMP-2 and MMP-9 production (Okuma et al., 2004).

Here, the BAL cell population of Hyp-DCHA-treated mice had a significantly lower percentage of PMNs (less than half that of untreated animals) 2 days after the bleomycin injury, at the time when the majority of the extravasated cell population is represented by PMNs (Kimura et al., 2006). Furthermore, histological staining and image analysis of lungs after 4 weeks have clearly shown that both the inflammatory cell infiltration and the patchy fibrosis were significantly reduced in animals given i.p. Hyp-DCHA. Moreover, although the former was reduced by 70% (Fig. 7, 1), the latter was inhibited even more (Fig. 7, 3). Quantitative determination of hydroxyproline (a marker of collagenous proteins) indeed revealed a reduction of more than 60% of collagen deposition, but the less pronounced result—compared with automated image analysis—may in part originate from the increased lung mass due to the inflammatory infiltrate, which, mostly in the untreated mice, lowers the estimated collagen relative content. This reduction was nevertheless statistically significant, despite bleomycin inoculation commonly resulting in a patchy distribution of the injury, and only a single lobe per mouse was analyzed. The efficacy of the treatment with Hyp-DCHA in containing the lung damage was paralleled by a regular weight gain of the animals.

The lung damage induced by bleomycin is rapid in onset, accompanied by early inflammation (Kimura et al., 2006), and followed by a complex process of repair at the site of injury. Our model took into consideration both the early inflammatory response (2 days) and the late fibrotic stage (28 days) of the bleomycin-induced lung injury, and the results show that hyperforin reduces both the early and late inflammatory responses as well as the fibrotic late stage. How much

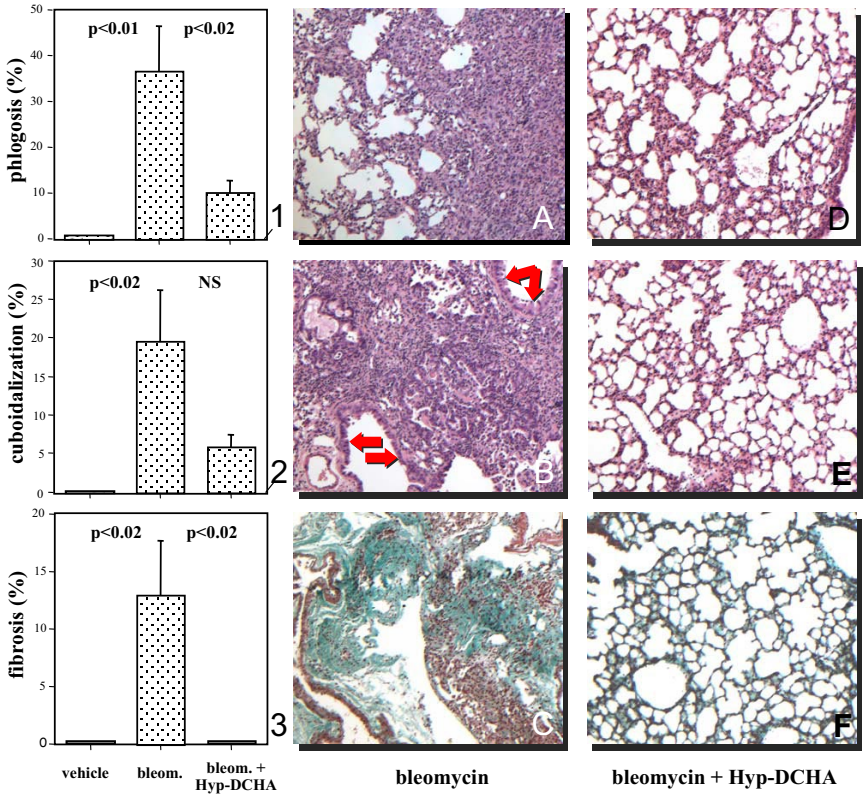

Fig. 7. Daily i.p. Hyp-DCHA protects mice from inflammation-triggered pulmonary fibrosis. Foci of inflammatory infiltration (A and B; H&E), cuboidalization of epithelial cells (arrows in B), and peribronchial and interstitial fibrosis (blue-green in C; Heidenhain trichrome) are clearly visible in example lungs of bleomycin-treated mice, whereas reduced or normal parenchyma is seen in bleomycin plus Hyp-DCHA-treated animals after 4 weeks (D and E: H&E; F: Heidenhain trichrome). All histologies are at 25× magnification. Image analysis quantitation confirms the reduction of bleomycin-induced phlogosis (histogram 1), cuboidalization (histogram 2), and fibrosis (histogram 3) in bleomycin- plus Hyp-treated mice. Each column represents the mean of eight fields per two sections per animal of each group.

the latter is due to the down-modulation of other cells (such as endothelial cells, as recently reported; Pacholok et al., 1995; Martinez-Poveda et al., 2005; Schempp et al., 2005) is yet to be determined. Certainly, this safe vegetable secondary metabolite is a good inhibitor of one of the most aggressive PMN proteases (LE) and may be effective in the treatment of individuals exposed to risk of excessive or chronic inflammation.

Recurrent inflammation is considered a causative step of tumoral transformation in some types of tissue, and inflammatory infiltration of the primary mass is common (Balkwill and Mantovani, 2001). Whether and to what extent the inhibition exerted by Hyp-DCHA on LE-triggered activation of MMP-9—also instrumental in cancer invasion—successfully contributes to checking tumor metastatic aggressiveness (Donà et al., 2004) is under investigation.

Acknowledgments

We are grateful to Prof. Giovanni Appendino for the generous gift of Hyp-DCHA, Dr. Giustina De Silvestro (Immuno-transfusion Service, Padova Hospital, Padova, Italy) for supplying buffy coats, Dr. Simona Minghelli (National Institute for Research on Cancer, Genova, Italy) for the histological analysis of neoangiogenesis, and Dr. Susan Biggin for revision of the English manuscript.

References

Balkwill F and Mantovani A (2001) Inflammation and cancer: back to Virchow? *Lancet* **357:**539–545.

Barnes J, Anderson LA, and Phillipson JD (2001) St. John's wort (*Hypericum perforatum* L.): a review of its chemistry, pharmacology and clinical properties. *J Pharm Pharmacol* **53:**583–600.

Benelli R, Barbero A, Ferrini S, Scapini P, Cassatella M, Bussolino F, Tacchetti C, Noonan DM, and Albini A (2000) Human immunodeficiency virus transactivator protein (Tat) stimulates chemotaxis, calcium mobilization, and activation of human polymorphonuclear leukocytes: implications for Tat-mediated pathogenesis. *J Infect Dis* **182:**1643–1651.

Benelli R, Morini M, Carrozzino F, Ferrari N, Minghelli S, Santi L, Cassatella M, Noonan DM, and Albini A (2002) Neutrophils as a key cellular target for angiostatin: implications for regulation of angiogenesis and inflammation. *FASEB J* **16:** 267–269.

Biber A, Fisher H, Romer A, and Chatterjee SS (1998) Oral bioavailability of hyperforin from *Hypericum* extracts in rats and human volunteers. *Pharmacopsychiatry* **31:**36–43.

Brolis M, Gambetta M, Fuzzati R, Pace R, Panzeri F, and Peterlongo F (1998) Identification by high-performance liquid chromatography-UV absorbance detection of active constituents of *Hypericum perforatum*. *J Chromatogr A* **825:**9–14.

Burdick MD, Murray LA, Keane MP, Xue YY, Zisman DA, Belperio JA, and Strieter RM (2005) CXCL11 attenuates bleomycin-induced pulmonary fibrosis via inhibition of vascular remodeling. *Am J Respir Crit Care Med* **171:**261–268.

Cervo L, Rozio M, Ekalle-Soppo CB, Guiso G, Morazzoni P, and Caccia S (2002) Role of Hyperforin in the antidepressant-like activity of *Hypericum perforatum* extracts. *Psychopharmacology* **164:**423–428.

Chatterjee SS, Erdelmeier C, Klessing K, Marmé D, and Schächtele C (1999) inventors: GMBH & CO, Ltd., Chatterjee SS, Erdelmeier C, Klessing K, Marmé D, and Schächtele C, assignees. Stable Hyperforin salts: method for producing them and their use in the treatment of Alzheimer's disease. World patent WO 99/41220. 1999 Aug 19.

Christensen P, Goodman L, Pastoriza B, Moore B, and Toews G (1999) Induction of lung fibrosis in the mouse by intratracheal instillation of fluorescein isothiocyanate is not T-cell-dependent. *Am J Pathol* **155:**1773–1779.

Corbel M, Belleguic C, Boichot E, and Lagente V (2002) Involvement of gelatinases (MMP-2 and MMP-9) in the development of airway inflammation and pulmonary fibrosis. *Cell Biol Toxicol* **18:**51–61.

Delclaux C, Delacourt C, D'Ortho MP, Boyer V, Lafuma C, and Harf A (1996) Role of gelatinase B and elastase in human polymorphonuclear neutrophil migration across basement membrane. *Am J Respir Cell Mol Biol* **14:**288–295.

Diaz-Gonzalez F, Gonzalez-Alvaro I, Campanero MR, Mollinedo F, del Pozo MA, Munoz C, Pivel JP, and Sanchez-Madrid F (1995) Prevention of in vitro neutrophil-endothelial attachment through shedding of L-selectin by non-steroidal anti-inflammatory drugs. *J Clin Investig* **95:**1756–1765.

Donà M, Dell'Aica I, Calabrese F, Benelli R, Morini M, Albini A, and Garbisa S (2003) Neutrophil restraint by green tea: inhibition of inflammation, associated angiogenesis, and pulmonary fibrosis. *J Immunol* **170:**4335–4341.

Donà M, Dell'Aica I, Pezzato E, Sartor L, Calabrese F, Della Barbera M, Donella-Deana A, Appendino G, Borsarini A, Caniato R, et al. (2004) Hyperforin inhibits cancer invasion and metastasis. *Cancer Res* **64:**6225–6232.

Dri P, Haas E, Cramer R, Menegazzi R, Gasparini C, Martinelli R, Scheurich P, and Patriarca P (1999) Role of the 75-kDa TNF receptor in TNF-induced activation of neutrophil respiratory burst. *J Immunol* **162:**460–466.

Esparza J, Kruse M, Lee J, Michaud M, and Madri JA (2004) MMP-2 null mice exhibit an early onset and severe experimental autoimmune encephalomyelitis due to an increase in MMP-9 expression and activity. *FASEB J* **18:**1682–1691.

Garbisa S, Biggin S, Cavallarin N, Sartor L, Benelli R, and Albini A (1999) Tumor invasion: molecular shears blunted by green tea. *Nat Med* **5:**1216.

Keane MP, Belperio JA, Moore TA, Moore BB, Arenberg DA, Smith RE, Burdick MD, Kunkel SL, and Strieter RM (1999) Neutralization of the CXC chemokine, mac-

rophage inflammatory protein-2, attenuates bleomycin-induced pulmonary fibrosis. *J Immunol* **162:**5511–5518.
Kimura T, Ishuu Y, Yoh K, Morishima Y, Iizuka T, Kiwamoto T, Matsuno Y, Homma S, Nomura A, Sakamoto T, et al. (2006) Overexpression of the transcription factor GATA-3 enhances the development of pulmonary fibrosis. *Am J Pathol* **169:**96–104.
Lee W and Downey GP (2001) Leukocyte elastase. Physiological functions and role in acute lung injury. *Am J Respir Crit Care Med* **164:**896–904.
Luscinskas FW, Ding H, and Lichtman AH (1995) P-selectin and vascular cell adhesion molecule 1 mediate rolling and arrest, respectively, of CD4+ T lymphocytes on tumor necrosis factor alpha-activated vascular endothelium under flow. *J Exp Med* **181:**1179–1186.
Lynam E, Sklar LA, Taylor AD, Neelamegham S, Edwards BS, Smith CW, and Simon SI (1998) Beta2-Integrins mediate stable adhesion in collisional interactions between neutrophils and ICAM-1-expressing cells. *J Leukoc Biol* **64:**622–630.
Martinez-Poveda B, Quesada AR, and Medina MA (2005) Hyperforin, a bio-active compound of St. John's wort, is a new inhibitor of angiogenesis targeting several key steps of the process. *Int J Cancer* **117:**775–780.
Moore BB, Paine R 3rd, Christensen PJ, Moore TA, Sitterding S, Ngan R, Wilke CA, Kuziel WA, and Toews GB (2001) Protection from pulmonary fibrosis in the absence of CCR2 signaling. *J Immunol* **167:**4368–4377.
Neri D and Bicknell R (2005) Tumour vascular targeting. *Nat Rev Cancer* **5:**436–446.
Okuma T, Terasaki Y, Kaikita K, Kobayashi H, Kuziel WA, Kawasuji M, and Takeya M (2004) C–C chemokine receptor 2 (CCR2) deficiency improves bleomycin-induced pulmonary fibrosis by attenuation of both macrophage infiltration and production of macrophage-derived matrix metalloproteinases. *J Pathol* **204:**594–604.
Pacholok SG, Davies P, Dorn C, Finke P, Hanlon WA, Mumford RA, and Humes JL (1995) Formation of polymorphonuclear leukocyte elastase: alpha 1 proteinase inhibitor complex and A alpha (1-21) fibrinopeptide in human blood stimulated with the calcium ionophore A23187. A model to characterize inhibitors of polymorphonuclear leukocyte elastase. *Biochem Pharmacol* **49:**1513–1520.
Quiney C, Billard C, Mirshahi P, Fourneron J-D, and Kolb J-P (2006) Hyperforin inhibits MMP-9 secretion by B-CLL cells and microtubule formation by endothelial cells. *Leukemia* **20:**583–589.
Rice WG and Weiss SJ (1990) Regulation of proteolysis at the neutrophil-substrate interface by secretory leukoprotease inhibitor. *Science (Wash DC)* **249:**178–191.
Sartor L, Pezzato E, and Garbisa S (2002) (−)Epigallocatechin-3-gallate inhibits leukocyte elastase: potential of the phyto-factor in hindering inflammation, emphysema, and invasion. *J Leukoc Biol* **71:**73–79.
Schempp CM, Pelz K, Wittmer A, Schopf E, and Simon JC (1999) Antibacterial activity of hyperforin from Saint John's wort, against multiresistant Staphylococcus aureus and Gram-positive bacteria. *Lancet* **353:**2129.
Schempp CM, Winghofer B, Ludtke R, Simon-Haarhaus B, Schšpf E, and Simon JC (2000) Topical application of St. John's wort (*Hypericum perforatum* L.) and of its metabolite hyperforin inhibits the allostimulatory capacity of epidermal cells. *Br J Dermatol* **142:**979–984.
Schempp CM, Kirkin V, Simon-Haarhaus B, Kersten A, Kiss J, Termeer CC, Gilb B, Kaufmann T, Borner C, Sleemann JP, et al. (2002) Inhibition of tumor cell growth by hyperforin, a novel anticancer drug from St. John's wort that acts by induction of apoptosis. *Oncogene* **21:**1242–1250.
Schempp CM, Kiss J, Kirkin V, Averbeck M, Simon-Haarhaus B, Kremer B, Termeer CC, Sleemann J, and Simon JC (2005) Hyperforin acts as an angiogenesis inhibitor. *Planta Med* **71:**999–1004.
Selman M, King TE, and Pardo A (2001) Idiopathic pulmonary fibrosis: prevailing and evolving hypotheses about its pathogenesis and implications for therapy. *Ann Intern Med* **134:**136–151.
Sternlicht MD and Werb Z (1999) Neutrophil elastase and cathepsin G, in *Extracellular Matrix, Anchor, and Adhesion Proteins* (Kreis T and Vale R eds) pp 543–545, Oxford University Press, Oxford, England.
Umezawa H (1976) Structures and activities of protease inhibitors of microbial origin. *Methods Enzymol* **45:**678–695.
Verotta L, Appendino G, Belloro E, Bianchi F, Sterner O, Lovati M, and Bombardelli E (2002) Synthesis and biological evaluation of hyperforin analogues. Part I. Modification of the enolized cyclohexanedione moiety. *J Nat Prod* **65:**433–438.
Zhou C, Tabb MM, Sadatrafiei A, Grün F, Sun A, and Blumberg B (2004) Hyperforin, the active component of St. John's wort, induces IL-8 expression in human intestinal epithelial cells via a MAPK-dependent, NF-kB-independent pathway. *J Clin Immunol* **24:**623–636.

Address correspondence to: Dr. Spiridione Garbisa, Department of Experimental Biomedical Sciences, viale G. Colombo 3, 35121 Padova, Italy. E-mail garbisa@unipd.it